Vision Res. Vol. 29, No. 8, pp. 989–1004, 1989
Printed in Great Britain.

0042-6989/89 $3.00 + 0.00

STEREOPSIS AND CONTRAST

GORDON E. LEGGE and YUANCHAO GU
Department of Psychology, University of Minnesota, 75 East River Rd, Minneapolis, MN 55455, U.S.A.

(*Received* 29 *December* 1987; *in revised form* 13 *December* 1988)

Abstract—We have measured threshold disparity as a function of the spatial frequency (0.25–20 c/deg) and contrast (0.02–0.75) of sine-wave gratings. In forced-choice trials, subjects indicated whether a target grating had crossed or uncrossed disparity relative to a reference grating. Thresholds were lowest near 3 c/deg and rose in proportion to spatial period at lower frequencies. Above 3 c/deg, there were marked individual differences. Across the range of spatial frequencies, disparity sensitivity and contrast sensitivity were correlated ($r = 0.84$). Threshold disparity was inversely proportional to the square root of contrast. When the contrast seen by one eye was reduced producing unequal monocular contrasts, threshold disparity rose more than when the contrast seen by the two eyes was reduced by the same amount. Our results have implications for stereo models that use zero crossings, peaks and troughs, or centroids as matching primitives. These models can account for the decline in disparity sensitivity at low sapatial frequencies but only the peak model satisfactorily accounts for the effect of contrast. If the limiting sources of noise in the two eyes are highly correlated, the effect of unequal monocular contrast can be accounted for using a differential-amplifier principle.

Stereopsis Contrast Spatial frequency

INTRODUCTION

There exists evidence that contrast has little or no effect on disparity sensitivity. Ogle and Weil (1958) required subjects to judge the depth of a test line located 0.5 deg to the right of a fixated test line. Variation of the intensity of the test line relative to the adapting background level had very little effect on stereoacuity. Lit, Finn and Vicars (1972) conducted the most thorough study of the effects of contrast on stereopsis. Subjects adjusted one vertical test bar to match the depth of a fixed bar. The targets were presented against an illuminated background. Light levels of both the background and the test bars were varied over a wide range. The authors concluded that contrast had no effect on stereoacuity as long as target light levels were sufficiently different (brighter or dimmer) from the background so that the targets were visible.

On the other hand, psychophysical models of contrast coding and electrophysiological data make it clear that internal visual response grows with stimulus contrast. The psychophysical models typically include a compressive nonlinearity for suprathreshold contrasts (Carlson & Cohen, 1978; Legge & Foley, 1980; Wilson, 1980; Burton, 1981; Legge, 1984). According to the Legge and Foley model, for example, internal visual response grows as the 0.4-power of suprathreshold stimulus contrast. Assuming that stereopsis relies on neural signals that increase with stimulus contrast, we should expect disparity sensitivity to improve with contrast. The expected relation between disparity sensitivity and contrast will depend on one's stereo model. We addressed this issue empirically by measuring the contrast dependence of disparity sensitivity for sine-wave grating targets. We compared our results with the predictions of stereo models that reply on spatial localization of zero crossings, peaks and troughs, and centroids in the response profiles of spatial-frequency channels.

Of crucial importance to steropsis is the matching problem. It has been argued that matching based on intensities or contrasts is unreliable and that primitives must be used that are immune to variations in these stimulus quantities (see, e.g. Poggio & Poggio, 1984). By this argument, we would expect disparity sensitivity to be little affected when unequal contrasts are presented to the two eyes. We asked how similar the monocular contrasts must be in order to support stereopsis. We measured disparity threshold as a function of interocular contrast ratio for sine-wave gratings.

Some previous findings suggest that unequal monocular contrasts adversely affect disparity sensitivity. Westheimer and McKee (1980a) and Wood (1983) compared the effects of monocular and binocular lens blur on stereo acuity. Simons (1984) made similar comparisons with blur caused by multiple layers of slightly hazy plastic bags. In these studies, monocular blur reduced stereo acuity as much or more than binocular blur. On the other hand, Julesz (1971, p. 96) has demonstrated that stereopsis can be sustained in the presence of substantial monocular blur in random-dot stereograms. Julesz, however, did not measure the effects on stereoacuity of contrast inequality.

We also studied the dependence of disaparity sensitivity on spatial frequency. Previous work suggests that good stereoacuity may not require high resolution. Stigmar (1971) measured stereoacuity for bright bars presented on a dark background. He used a ground-glass diffuser to produce blur. He characterized blur by the width at half height of the light distributions produced by the diffuser. Stereoacuity did not decrease until these widths exceeded 4.5 min. If we characterize ground-glass blur as Gaussian low-pass filtering, Stigmar's figure of 4.5 min corresponds to a 1/e filter bandwidth of about 7 c/deg. His results imply that stereoacuity does not benefit from spatial frequencies above 7 c/deg. Westheimer and McKee (1980a) measured stereoacuity for line targets after several forms of spatial-frequency filtering. They found that high-pass filtering was more detrimental to stereoacuity than low-pass filtering, although all forms of filtering elevated thresholds. Schor and Wood (1983) measured stereo thresholds for difference-of-Gaussian (DOG) targets. Thresholds were constant for center frequencies ranging from about 2.5 to 19 c/deg. Below 2.5 c/deg, thresholds were proportional to the center width of the DOG target.

Recent influential stereo models propose localization and matching of spatial features within channels and some form of coupling across channels. Our sine-wave data enabled us to study the localization process at different scales relatively free of cross-channel interactions. Another reason for studying frequency effects was to look for a link between contrast sensitivity and disparity sensitivity. There is evidence for such a link in the work of Frisby and Mayhew (1978). They observed that contrast thresholds for detecting fixed disparity in narrow-band-filtered random-dot stereograms were nearly constant at 0.3–0.4 log units above contrast-detection threshold in the range 2.5–15 c/deg.

METHOD

Apparatus and stimuli

Gratings were produced on a Joyce Electronics CRT display. The display had a desaturated green P-31 phosphor and a mean luminance of 340 cd/m^2.

As illustrated in Fig. 1, the display was comprised of four panels. An opaque black divider bisected the screen vertically and extended to the subject's nose. As a result, each eye saw only the pair of panels on its side of the divider. Each panel measured 11.3 cm horizontally by 7 cm vertically. Upper and lower panels were separated by horizontal opague strips 1.25 cm wide, with fixation spots at the center. Lenses and prisms to aid convergence and accommodation were held in trial frames mounted on the end of the divider. The bottom pair of panels formed one stereo image and the top pair another.

Vertical sinewave gratings were generated digitally with an LSI-11/23 computer. A 1024-point waveform representing one cycle of a sinewave was stored in computer memory. To produce a sine-wave grating, the waveform was sampled in regular steps with wrap-around, and the values were passed to a 12-bit digital-to-analog converter (D/A). The output of the D/A was passed to a 12-bit dB programmable attenuator. Separate D/A's produced the patterns on the top and bottom of the screen. A high-bandwidth switch, controlled by a pulse with adjustable delay, was used to switch between the two D/A's at the middle of each of the CRT's vertical raster lines. The switch output was applied to the CRT's Z-axis input. Spatial frequency was determined by the step size through the 1024-point waveform. Phase could be adjusted to one part in 1024 by specifying the starting point within the stored waveform. Contrast was controlled by the dB attenuator. Spatial frequency, contrast and phase could be specified independently in each of the four panels of the display. The pattern in each panel was constructed from 320 samples. The computer's D/A routines were synchronized with the CRT's sweep (100 Hz frame rate and 100 kHz raster frequency).

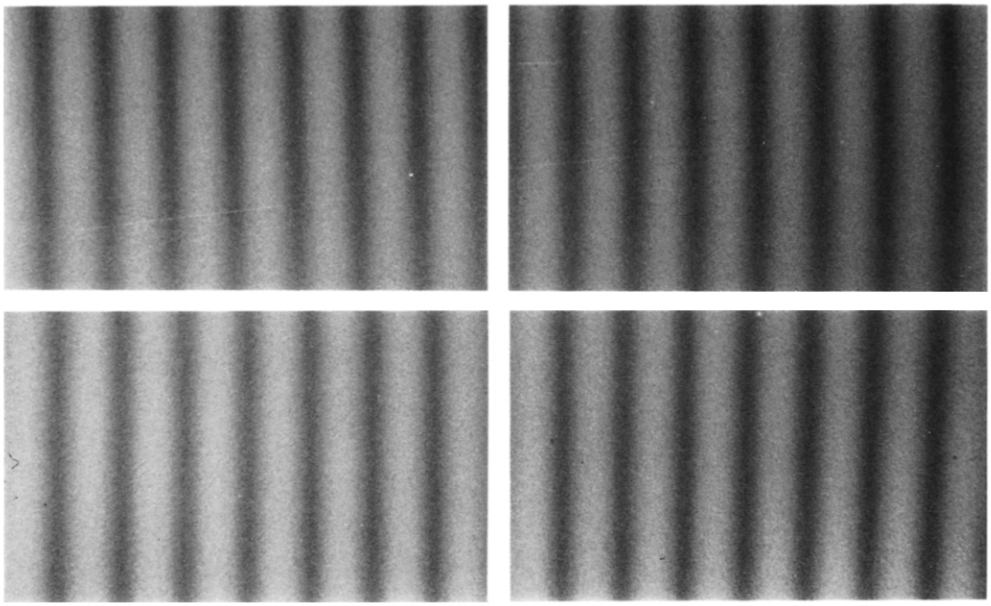

Fig. 1. Photograph of the four-panel CRT display. In the experiments, subjects' left and right eyes saw only the left and right pairs of panels respectively. The pair of sine-wave gratings in the bottom panels formed a *reference* stimulus having zero disparity. The pair of gratings in the top panels formed a *target* with crossed or uncrossed disparity (uncrossed in this photo).

The bottom pair of gratings formed a *reference* stimulus that always had zero disparity. The top pair of gratings formed the *target*. The target gratings were identical to the reference gratings except for phase. By introducing equal and opposite phase shifts in the left and right members of the stereo pair, we created crossed or uncrossed disparity along the midline. In Fig. 1, the gratings in the top pair are phase-shifted outward from the fixation points. The fused image of this target would appear to lie behind the reference pattern. This is an example of uncrossed disparity. Throughout this paper, we express disparity as an angle – twice the visual angle associated with the phase shift in each component.

Measurements were made for the following viewing distances and spatial frequencies: 57 cm (0.25 and 0.5 c/deg), 2 m (1.5–5.0 c/deg), 4 m (7.5 and 10 c/deg) and 8 m (15 and 20 c/deg). In one experiment, stereo thresholds were measured for square-wave rather than sine-wave gratings. All square-wave thresholds were obtained at 8 m except for the 0.5 c/deg threshold which was obtained at 4 m.

Procedure

Stimuli were presented continuously until a subject responded within a forced-choice trial. Subjects fused the left and right fields but were permitted to move their eyes off the fixation points. The reference pattern always had zero disparity and the target's disparity was selected at random from a set of 13 values: six uncrossed, six crossed, and one with zero disparity. The subject pressed a button indicating whether the target was in front of or behind the reference. Feedback was provided.

Raw data from each session consisted of separate psychometric functions for crossed and uncrossed disparity, with proportion correct as a function of disparity. The data were fit by functions of the form:

$$d' = (D/D_0)^n. \quad (1)$$

d' is computed as $\sqrt{2}$ times the standard deviate associated with proportion correct (Green & Swets, 1974), D is disparity, and D_0 is the disparity threshold. It is defined as the disparity for which $d' = 1$ (corresponding to about 76% correct). The parameter n indicates the steepness of the psychometric function. Maximum-likelihood estimates were found for D_0 and n. χ^2 tests indicated that equation (1) usually provided a good fit to the data. Each psychometric function was based on about 500 trials. Mean thresholds and slopes were based on at least four psychometric functions. Data sets were excluded from analysis when overall performance was less than 67% correct (indicating an inappropriately low range of disparities), when the slope estimate was less than 0.4 or the χ^2 fit was bad (indicating highly nonmonotonic psychometric functions producing spurious threshold estimates). Exclusion of data sets was rare once a disparity range was located that spanned threshold.

Catch trials where the target had zero disparity were included to check for response bias. Occasionally, subjects exhibited bias, giving more of one type of response than the other. Such a bias tends to lower the estimated threshold and slope for disparities of one sign, and raise them for disparities of the opposite sign. Using the score on the catch trials as an estimate of bias, we corrected the proportions in the remaining conditions. Suppose that in the catch trials, the subject responds "crossed" with proportion x. Let P_{obs} be the observed proportion correct for some nonzero crossed disparity. According to a classical guessing model, the corrected proportion P_c is:

$$P_c = 0.5\,(P_{obs} - x)/(1 - x) + 0.5 \quad (x > 0.5) \quad (2)$$

$$0.5\,(P_{obs} - 1)/x + 1 \quad (x < 0.5).$$

Equation (2) was used to correct the observed proportions for response bias. Generally, the bias was small and the correction had small effects.

In one series of experiments, unequal contrasts were presented to the two eyes. Data for four psychometric functions were collected in interleaved fashion within a session: crossed and uncrossed disparities and higher contrast presented to the left or right eye. The same curve-fitting procedures were used to estimate thresholds and slopes from these functions, but each of the four functions was based on only three disparities. In all such experiments, the higher contrast was either 0.125 or 0.25.

In one set of experiments, briefly reported in this paper, the subject saw only a single stereo image, lying in the plane of fixation. Midway through a 1 sec exposure interval, the sine-wave grating target was displaced along the midline by introducing crossed or uncrossed disparity. The subject reported the direction of the displacement.

Subjects

Seven subjects participated in the experiments. Stereoacuity was normal for all subjects as measured by the Orthorator Vision Tester and random-dot stereograms (Julesz, 1971).

We measured monocular (with the other eye occluded by an eye patch) and binocular contrast-sensitivity functions at a 4 m viewing distance. We used a spatial two-alternative forced-choice procedure in which a vertical grating appeared on either the left or right side of the CRT display (with no divider present). The subject indicated which side contained the grating. The subject's contrast threshold (criterion of 75% correct) was estimated using the QUEST staircase procedure (Watson & Pelli, 1983). No subjects showed systematic interocular differences in contrast sensitivity.

RESULTS AND DISCUSSION

Each panel of Fig. 2 shows examples of psychometric functions for crossed and uncrossed disparity. The targets were 0.5 and 2.5 c/deg sine-wave gratings.

The data in each panel were collected in one session. Detectability d' is plotted against disparity, both on log scales, and the best-fitting straight lines have been drawn through each set of data. Threshold is defined as the disparity for which the fitted line has a d' value of 1.

There were small individual differences in sensitivity to crossed and uncrossed disparity. KD exhibited the largest effect. Averaged across 42 sessions, her thresholds for uncrossed disparity were 18.5% higher than for crossed disparity. By comparison, DR, for whom we have the most comprehensive data, had average thresholds for crossed disparity that were 5.86% higher than those for uncrossed disparity. Data points in the subsequent figures represent geometric means of at least four threshold estimates (both crossed and uncrossed).

Slopes of psychometric functions are sometimes of theoretical interest. Table 1 lists some representative values. Here, mean slopes are given for data collected at two spatial frequencies and several contrasts for one subject. (Corresponding threshold data are shown in Fig. 6). The slopes are close to one for the 3.5 c/deg data and a little lower at 0.5 c/deg. Overall, slopes tended to be close to, but a little less than one.

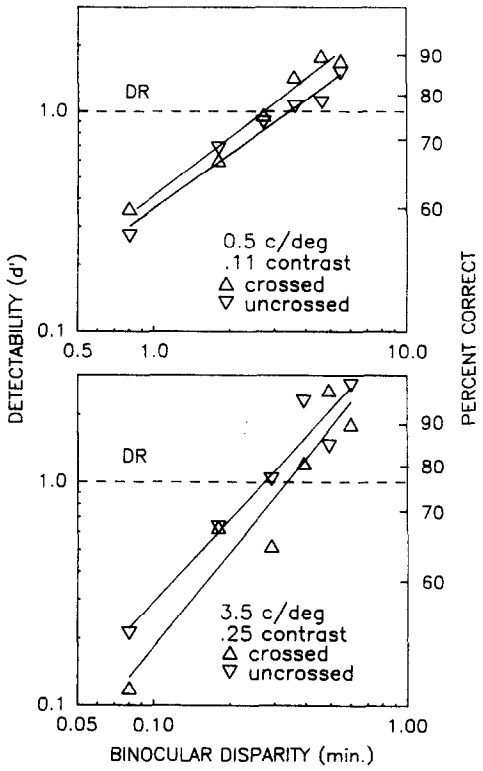

Fig. 2. Illustrative psychometric functions. Detectability (left ordinate) and percent correct (right ordinate) are plotted as a function of disparity for fixed values of crossed and uncrossed target disparity. Each panel summarizes results from one session comprised of about 1000 trials. Threshold is defined as the disparity for which the fitted straight lines have unit detectability ($d' = 1$).

Effect of spatial frequency

Figure 3 shows threshold disparity as a function of spatial frequency for four subjects—solid circles for a contrast of 0.25 and open circles for a contrast of 0.03. First notice that all of the curves for sine-wave targets have a descending branch at low frequency extending to a

Table 1. Mean slopes of psychometric functions for DR

0.5 c/deg			3.5 c/deg		
Contrast	Slope	SE(%)	Contrast	Slope	SE(%)
0.0224	0.57	14	0.03	0.91	8
0.05	0.81	14	0.09	0.96	7
0.11	0.85	5	0.25	1.32	7
0.25	0.81	25	1.0	0.82	7
0.73	0.71	23			

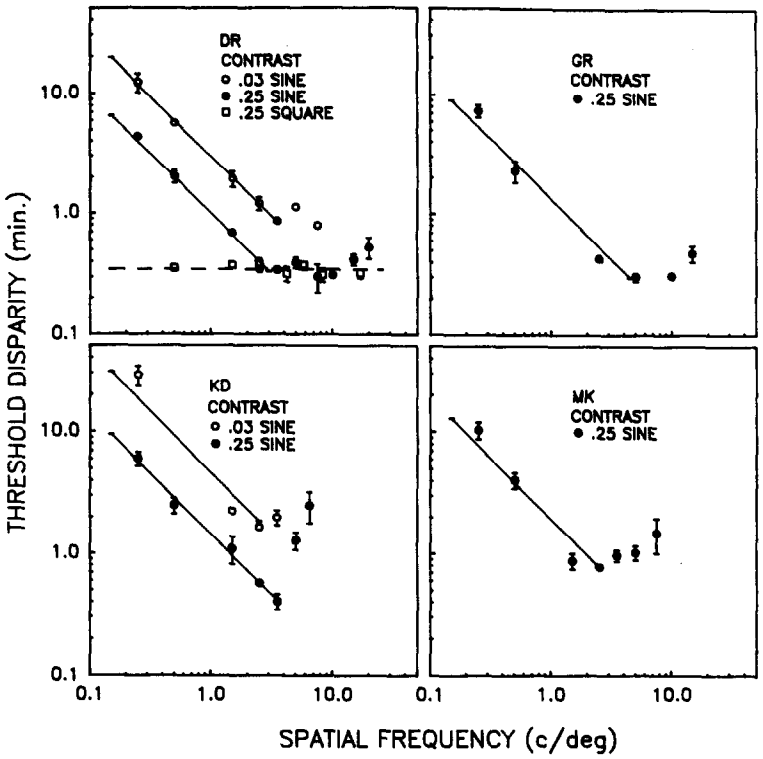

Fig. 3. Threshold disparity as a function of spatial frequency. The four panels show mean thresholds and standard errors for four subjects. The solid lines have slopes of −1.0. (Table 2 lists slopes of best-fitting straight lines.) The horizontal dashed line at 0.344′ in DR's panel shows the mean threshold disparity for 0.25-contrast square-wave targets. All other data refer to sine-wave grating stimuli.

minimum near 3 c/deg. A slope of −1.0 fits the descending branch. Best-fitting lines have slopes ranging from −0.98 to −1.29 (see Table 2). Along this descending branch, disparity thresholds are inversely proportional to spatial frequency. This scaling may be expressed as a constant phase shift in the sinusoidal components of the target. For 0.25-contrast sine-wave targets, the constant monocular phase shift at disparity threshold ranged from 2.9 deg for DR to 6.4 deg for MK (see Table 2). Schor and Wood (1983) obtained a constant monocular phase shift of 3 deg for their 100%-contrast, low-frequency DOG targets.

Figure 3 shows that the best stereopsis for gratings occurs for medium frequencies, around 3 c/deg, and does not require high spatial resolution. This result is consistent with Stigmar's (1971) finding that stereoacuity is quite resistant to ground-glass blur.

Two control experiments revealed that the low-frequency branch is not an artifact related to changes in viewing distance. First, the angular subtense of the horizontal strip separating target and reference stimuli decreased from 1.25 to 0.36 deg as viewing distance increased from 57 cm to 2 m. Both Berry (1948) and Westheimer and McKee (1980b) have shown that vertical separation affects stereo thresholds. Their data indicate that the threshold is lowest near 0.1–0.2 deg, with some indication of a rise for greater separations. We measured KD's

Table 2. Disparity thresholds at low spatial frequency: slopes and constant monocular phase shifts

Subject	Contrast	Spatial frequency range (c/deg)	Slope	Monocular phase shift at threshold (deg)
KD	0.25	0.25–3.5	−0.98	4.3
	0.03	0.25–2.5	−1.29	13.8
MK	0.25	0.25–2.5	−1.10	6.4
DR	0.25	0.25–2.5	−1.10	2.9
	0.03	0.25–3.5	−1.02	8.9
GR	0.25	0.25–5.0	−1.05	4.1

disparity threshold as a function of target-reference separation (0.32–4.4 deg) for 0.5 c/deg sine-wave gratings viewed from 57 cm, and (0.09–1.25 deg) for 2.5 c/deg gratings viewed from 2 m. There were no significant effects of separation on disparity threshold. Second, the number of grating cycles in the targets increased with increasing spatial frequency despite changes in viewing distance, ranging from about 3 cycles at 0.25 c/deg to about 9 cycles at 3 c/deg. In a control experiment with MK, we measured disparity threshold as a function of the number of grating cycles (2–6) for 0.5 c/deg targets at a viewing distance of 57 cm. Threshold decreased by 11% across this range but this effect was not significant. We conclude that neither target-reference separation nor the number of stimulus cycles had much effect on the shapes of the curves in Fig. 3.

Figure 3 illustrates a different pattern of results above 3 c/deg; thresholds level out or rise. There is substantial individual variation. At a contrast of 0.25, DR shows a plateau in which disparity thresholds for sine-wave targets are nearly constant from 2.5 to 15 c/deg. GR shows a plateau of shorter extent, but thresholds for KD and MK begin to rise immediately. The high-frequency rise in thresholds is quite rapid. The rightmost data point for each curve in Fig. 3 represents the highest spatial frequency for which thresholds could be measured reliably.

One factor that may limit sensitivity at high frequency is the periodicity of the sine-wave target itself. Periodic targets can be fused in multiple depth planes—the wallpaper illusion. In the case of a sine-wave grating, small monocular phase shifts simulating small crossed disparity are equivalent to large phase shifts in the opposite direction producing a large uncrossed disparity. It is clear from our data that our subjects were able to distinguish easily between these alternatives. However, for high spatial frequencies threshold disparities corresponded to larger monocular phase shifts and hence greater potential ambiguity. This, coupled with fixational disparity of the eyes, may have played a role in the rapid high-frequency rise of disparity thresholds.

The shapes of the sine-wave curves in Fig. 3 are similar to disparity-threshold curves obtained with high-contrast DOG targets by Schor and Wood (1983). There is also an interesting resemblance to curves measured by Levi and Klein (1983). Their task was not stereo but one in which subjects set a line to bisect the interval between regularly spaced lines in a grating pattern. As in Fig. 3, localization thresholds dropped linearly with increasing spatial frequency to about 2 c/deg and were flat to higher spatial frequencies. In another hyperacuity task, Westheimer (1978) found that the displacement threshold for high-contrast sinusoidal gratings was constant from 3 to 25 c/deg at about 0.16 min (= 10 sec). This value is very close to the monocular displacement of 0.15 min associated with the high-frequency plateau in DR's data from 2.5 to 15 c/deg.

It is natural to ask whether contrast detection and disparity detection are related. Figure 4 shows contrast-sensitivity functions for the same subjects whose data are shown in Fig. 3. Campbell and Robson (1968) observed that the rolloff below the peak of the CSF had near-unity slope. Except for MK, our slopes were quite close to one (1.01, 0.94, 0.77 and 0.56 for DR, KD, GR and MK respectively). These values correspond to slopes near −1 for plots of contrast-detection threshold vs frequency, the same slope found in Fig. 3 for disparity. Moreover, the peaks of our CSFs occur at 4 c/deg, in rough correspondence to the minima in our disparity curves.

Figure 5 is a scatter plot in which each symbol shows corresponding values of contrast sensitivity and disparity threshold at one spatial frequency for one subject. The regression line through the data has a correlation coefficient of 0.84. Points obtained at different spatial frequencies are distinguished by symbol shape. Correlation coefficients at the different spatial

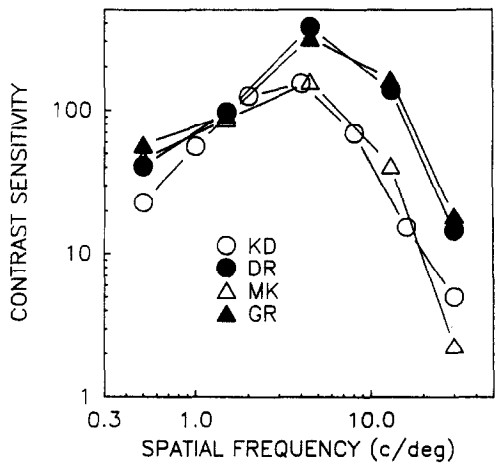

Fig. 4. Binocular contrast sensitivity functions for the four subjects whose disparity thresholds are given in Fig. 3.

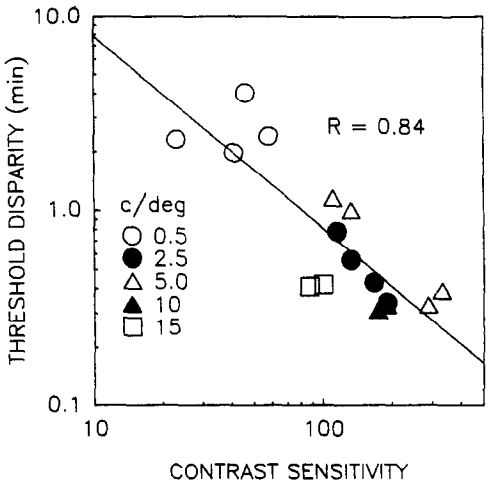

Fig. 5. Scatter plot illustrating the link between disparity thresholds and contrast sensitivities for sine-wave gratings. Each point represents the disparity threshold and corresponding contrast sensitivity (interpolated where necessary) at one spatial frequency for one subject. The correlation coefficient is 0.84. Correlation coefficients for the separate spatial frequencies are: 0.21 at 0.5 c/deg, 0.87 at 2.5 c/deg, 0.92 at 5 c/deg and 1.0 at 10 and 15 c/deg. (Values of 1.0 occurred because only two of the four subjects could do the stereo task at the high spatial frequencies.)

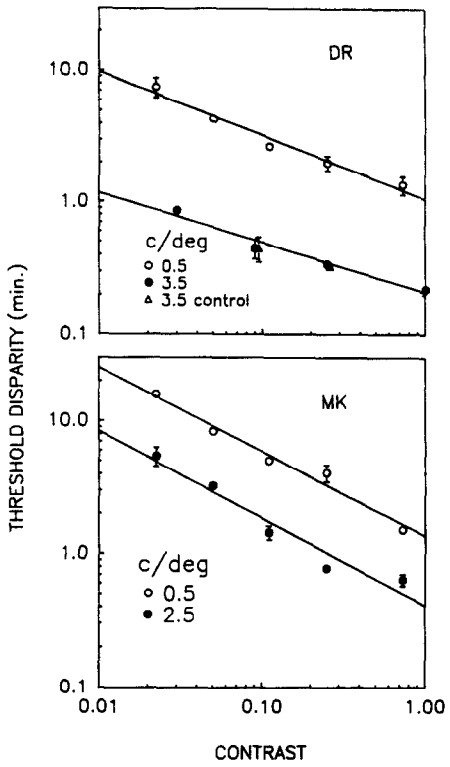

Fig. 6. Threshold disparity as a function of contrast. The two panels show mean threshold disparities and standard errors for two subjects. The results can be summarized by the slopes of best-fitting straight lines through the data. Slopes for the two subjects shown here and four others are given in Table 3. Data represented by triangles in DR's panel are results of a control experiment in which random lateral shifts were superimposed on the target gratings (see text).

frequencies are also high except at 0.5 c/deg. These values are given in the figure caption. The results in Fig. 5 suggest that suprathreshold disparity sensitivity is related to contrast sensitivity across a substantial range of spatial frequencies.

One set of square-wave data is shown for comparison with the sine-wave data in the upper-left panel of Fig. 3. The curve does not rise at low frequencies but is flat at a mean threshold value of 0.34 min from 0.5 to 17 c/deg.

The effect of contrast

Figure 6 shows threshold disparity as a function of sine-wave contrast at two spatial frequencies for DR and MK.

There is a gradual drop in disparity threshold as contrast rises. The slopes of best-fitting lines in log–log coordinates have values near −0.4 for DR and −0.6 for MK. These numbers represent exponents of power-function relations between disparity threshold and contrast. Exponents for six subjects are listed in Table 3. The entries for DP and GD summarize data collected with a stereo-displacement technique (see Method). The exponents in Table 3 cluster near −0.5 (geometric mean = −0.52, SE = 9%). This means that threshold disparities for gratings have an approximately inverse square-root dependence on contrast. Vernier acuity is another form of hyperacuity that shows a square-root dependence on contrast (Krauskopf & Campbell, unpublished data; Watt & Morgan, 1983; Morgan & Regan, 1987). Wilson (1986) found a slightly stronger dependence (mean exponent = −0.80).

Can we reconcile our findings with the results of Lit et al. (1972) who concluded that contrast

Table 3. Disparity thresholds as a function of contrast: slopes

Subject	Spatial frequency (c/deg)	Contrast range	Slope
KD	0.5	0.03–0.25	−0.84
	2.5	0.03–0.25	−0.47
MK	0.5	0.022–0.73	−0.63
	2.5	0.022–0.73	−0.66
DR	0.5	0.022–0.73	−0.47
	3.5	0.03–1.0	−0.38
TT	2.5	0.12–0.75	−0.48
GD[a]	0.5	0.11–0.73	−0.38
DP[a]	0.5	0.022–0.73	−0.54
		Mean = −0.52	
		SE = 9%	

[a]Stereo displacement thresholds, see Method.

Table 4. Effect of contrast on stereoacuity: reanalysis of the data of Lit et al. (1972)[a]

Background illuminance (log td)	Bright		Dark	
	Contrast range	Exponent	Contrast range	Exponent
−1.22	0.35–0.999	−2.6	0.20–0.93	−0.37
−0.57	0.19–0.999	−0.845	0.31–0.99	−0.81
1.02	0.26–0.99	0.125	0.25–0.98	−0.93
1.57	0.15–0.987	0.189	0.35–0.986	−0.91
2.06	0.22–0.96	0.103	0.20–0.988	−0.33

[a]Data in Fig. 2 of Lit et al. (1972) were reanalyzed. Stereoacuity was tabulated as a function of the Michelson contrast of the target lines. Best-fitting straight lines in log–log coordinates were computed. Slopes of these lines, representing power-function exponents, are listed in this table.

had virtually no effect on stereoacuity? Lit et al. graphed stereoacuity as a function of background and target light levels, not as a function of contrast. We reanalyzed their data to tabulate stereoacuity as a function of the Michelson contrast of the targets. [Michelson contrast is defined as $(L_t - L_b)/(L_t + L_b)$ where L_t and L_b are target and background luminances. Legge & Kersten (1983) have argued that this is the most parsimonious definition of contrast for light and dark bars.] We computed best-fitting power functions for plots of disparity threshold as a function of target contrast. Table 4 summarizes the exponents. The column headed "Dark" refers to cases in which targets were dimmer than the background and "Bright" to cases in which targets were brighter than the background. The table shows that for dark targets, stereo thresholds declined as target contrast rose with exponents ranging from −0.33 to −0.93. The results are mixed for bright bars with exponents ranging from −2.6 to +0.189. This reanalysis shows that the data of Lit et al. (1972) are at least consistent with a weak dependence of stereoacuity on contrast.

In a control experiment we asked whether subjects based their decisions on a *monocular cue*, the direction of monocular phase shifts. We added equal right (or left) phase shifts of random size to the left- and right-monocular gratings, simulating lateral shifts of the image. These added phase shifts masked the monocular cues to the sign of the disparity. As illustrated by the triangles in Fig. 6, thresholds were unchanged by the lateral shifts, confirming that subjects based their judgments on disparity.

Effect of unequal contrast

In the two panels of Fig. 7, disparity thresholds for DR and KD are plotted against *contrast ratio*. For each subject, there is one set of data at 2.5 c/deg and two sets at 0.5 c/deg. Within a set, the higher contrast was constant (either 0.125 or 0.25).

The lowest thresholds occurred at or near the 1:1 ratio and the curves are roughly symmetrical about this value. The curves all rise with growing steepness as the contrast ratio departs from 1:1.

Contrast ratio has a stronger effect on disparity sensitivity than does overall contrast. For example, DR's disparity threshold rose by a factor of 2.17 when overall contrast (i.e.

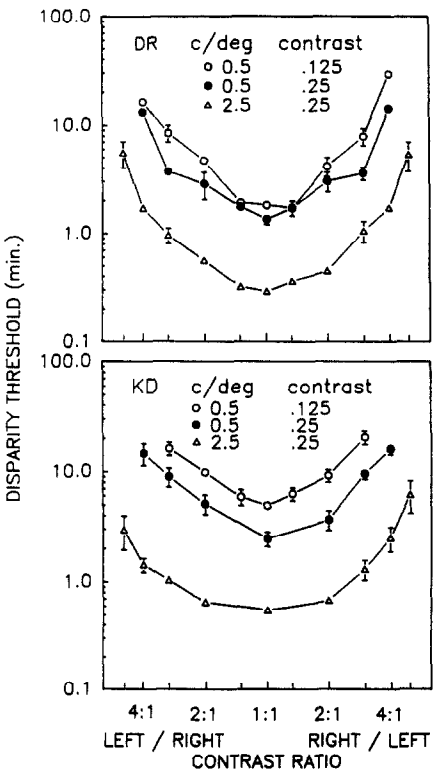

Fig. 7. Disparity thresholds as a function of contrast ratio. The horizontal axis shows the ratio of contrasts seen by the two eyes on a log scale. Regardless of the ratio, the higher contrast was always fixed at either 0.125 or 0.25 as indicated on the figure. Data are shown for observers DR and KD at two spatial frequencies.

both eyes) decreased from 0.25 to 0.05 at 0.5 c/deg, but by a factor of 10 when the contrast in just one eye decreased by about the same amount.

The results for unequal contrast are in qualitative agreement with findings cited earlier (Westheimer & McKee, 1980a; Wood, 1983; Simons, 1984). There is a problem, however, in reconciling these data with dichoptic masking data (Legge, 1979). In that study, subjects had to detect a signal grating presented to one eye in the presence of a same-frequency high-contrast masker grating in the other eye. The masking effect was surprisingly strong. In some cases, the signal's contrast at threshold was 50% of the masker's contrast. Given this result, we might expect stereopsis to be impossible when the ratio of monocular contrasts exceeds 2:1. This is not the case. Disparity detection was possible for contrast ratios of 3:1 and greater, albeit with reduced sensitivity. How do we account for this difference? In the dichoptic experiments, signal and masker were always in identical cosine phase with fixation (0 disparity) so disparity afforded no cue for detection. There is evidence from adaptation and noise-masking experiments for disparity-selective channels (Felton, Richards & Smith, 1972; Blakemore & Hague, 1972; Rubin, 1983). It is possible that signal detection in the dichoptic-masking experiment required discrimination of responses within a single disparity-selective channel while the disparity discrimination studied in the present paper involved comparison of responses from two or more such channels.

The results of Fig. 7 raise a question of some clinical interest. Typically, people with marked differences of contrast sensitivity in the two eyes show disruptions in stereopsis. Perhaps this is so because the "effective contrast" (i.e. suprathreshold contrast) is different in the two eyes, and these subjects are attempting stereopsis with an effective contrast ratio quite different from 1:1. If so, their stereopsis should improve if enhanced contrast is presented to the eye with reduced contrast sensitivity.

We conclude this subsection by constructing iso-sensitivity contours for grating stereopsis. We use the 0.5 c/deg data of Fig. 7 to find pairs of left-eye and right-eye contrasts having the same disparity thresholds. Contours are plotted for DR and KD in Fig. 8. These contours are nearly straight lines. This figure illustrates an effect reminiscent of Fechner's paradox. Increasing the contrasts seen by the two eyes does not necessarily improve disparity sensitivity. If the contrast ratio is allowed to depart from 1, sensitivity may stay the same or decline with increasing contrast.

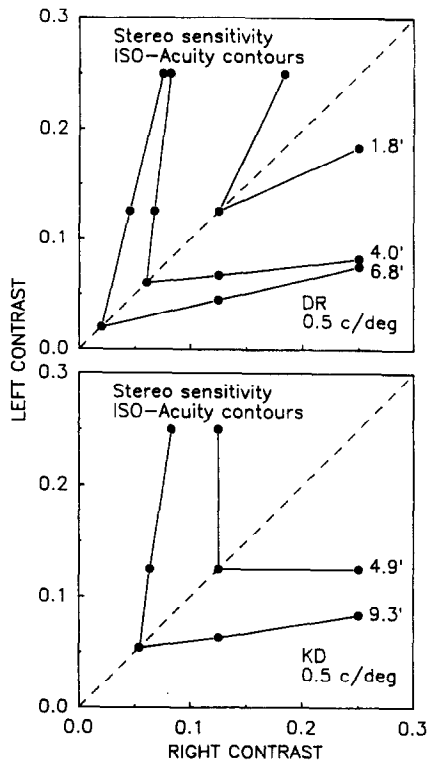

Fig. 8. Iso-sensitivity contours for grating stereopsis. Horizontal cuts through the 0.5 c/deg curves in Fig. 7 were used to find pairs of left-eye and right-eye contrasts having the same threshold disparities. In addition, curves like those in Fig. 6 were used to find the target with equal monocular contrasts having the same disparity threshold. These pairs of values are plotted as iso-sensitivity contours for DR and KD.

Comparison with the results of Halpern and Blake

Halpern and Blake (1988) have independently conducted experiments similar to ours. Despite some methodological differences, the studies are in fair empirical agreement where direct comparison is possible.

Halpern and Blake used D10 stimuli (10th derivatives of Gaussian luminance profiles) which are very similar to sine-wave gratings. In their first experiment, they measured the effect of contrast on disparity threshold at four spatial frequencies—1.2, 2.4, 4.8 and 9.6 c/deg. Contrasts ranged from 6 to 21 dB above the appropriate contrast-detection threshold. We varied contrast over a wider range at 0.5 c/deg and at either 2.5 or 3.5 c/deg (depending on the subject). The most direct comparison is with

Halpern and Blake's data at 2.4 c/deg. They found power function exponents relating disparity threshold to contrast having values of −0.31, −0.37 and −0.66 for three subjects. As listed in our Table 3, we found values of −0.47, −0.66 and −0.48 (2.5 c/deg) and −0.38 (3.5 c/deg). These results are in good agreement. Halpern and Blake found that mean exponent values decreased from low to high spatial frequency. We found no such effect, but our measurements spanned a lower range of spatial frequencies.

Halpern and Blake's second experiment was devoted to studies of unequal contrast. In an experiment analogous to ours, one eye received a fixed, high-contrast target. Disparity threshold was measured as a function of the contrast presented to the other eye. Once again, the best comparison can be made between their data at 2.4 c/deg and ours at 2.5 c/deg. They fixed the high-contrast grating at 21 dB above detection threshold, roughly a contrast of 0.11. Contrasts in the other eye ranged down to about 0.02 for a maximum contrast ratio near 5.5:1 (15 dB). Mean threshold disparity changed by a factor of about five. In our 2.5 c/deg experiment, the higher contrast was fixed at 0.25. Reduction of the contralateral monocular contrast to 0.0625 (i.e. a contrast ratio of 4:1) resulted in elevation of threshold disparity by factors of 5.86 and 3.36 for DR and KD respectively. The effect of contrast ratio is a little larger in our case, but the two studies are in fairly close agreement. Both studies found greater effects of contrast ratio at lower spatial frequencies (at 1.2 c/deg for Halpern and Blake, and 0.5 c/deg for us).

THEORETICAL IMPLICATIONS

Disparity detection requires the selection and interocular matching of appropriate monocular features. While the matching problem is of fundamental importance to stereo, the choice of features and the accuracy of their localization will limit disparity sensitivity.

According to most current models of spatial localization, stimuli are first filtered through linear band-pass spatial frequency channels.

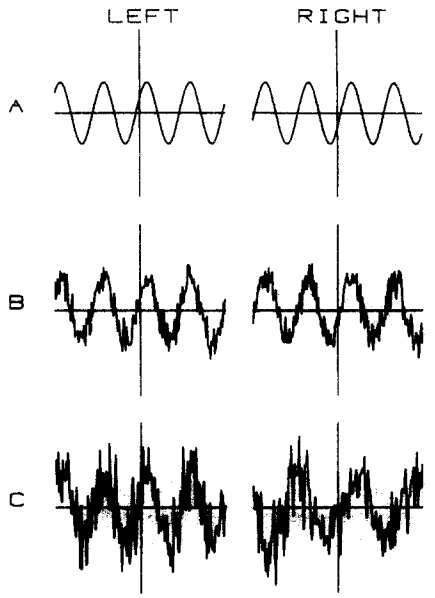

Fig. 9. Illustration of sinewaves perturbed by Gaussian noise. The left and right sinewaves have phase shifts of equal size but opposite direction, representing disparity along the midline. (A) In the absence of noise, the sinewave's zero crossings can be localized with unlimited accuracy. (B) When the noise standard deviation is small compared with the sine-wave amplitude, small clusters of zero crossings are found in the vicinity of the true zero crossings. The noise limits the precision with which the true zero crossings can be localized. (C) When the noise standard deviation is large compared with the sinewave's amplitude, the true zero crossings are very difficult to localize.

If the input is a sinewave grating, the filter's output is a sinusoidal waveform which we conceive to be a neural representation of the stimulus. Figure 9 illustrates the neural waveforms associated with sinewave gratings having equal but opposite phase shifts d, i.e. a disparity of $2d$.

What features of these neural waveforms are localized in detecting disparity? We will consider three proposed "spatial primitives:" zero crossings (Marr & Poggio, 1979), peaks and troughs (Mayhew & Frisby, 1981), and centroids* (Watt & Morgan, 1985).

In the absence of noise (Fig. 9A), each of these features can be localized with arbitrary accuracy. But suppose the neural waveforms are perturbed at each point by independent samples of Gaussian noise. In Fig. 9B the signal-to-noise ratio is much higher than in 9C, but in both cases the noise will limit the accuracy with which a candidate feature can be localized. Of the authors cited, only Watt and Morgan have considered how noise limits visual localization, and they have not done so for the case of stereopsis. The Marr and Poggio (1979)

*For a function $f(x)$ with adjacent zero crossings at a and b, the centroid of the zero-bounded region between a and b is the point about which the first-order moment is zero and is computed as

$$\int_a^b xf(x)\,dx \Big/ \int_b^a f(x)\,dx.$$

algorithm specifies the *largest* disparity that can be fused, but it has no means for specifying the smallest disparity that can be detected.

The noisy data in the neural waveform must be used to estimate the location of the spatial primitive. Mean accuracy of localization depends on the distribution of these estimates. We refer to this distribution as the *location distribution*. If the location distribution is broad, i.e. has a large standard deviation, accuracy of localization is low. Our goal in the following paragraphs is to ask how the SD of the location distributions for zero crossings, peaks and centroids depend on contrast and spatial frequency.

The noisy neural waveform contains an odd number of zero crossings in a tight cluster marking the location of each stimulus zero crossing (Fig. 9B). The sign of the stimulus zero crossing (positive or negative slope) is the same as the majority of the zero crossings in the cluster. Once the sign is determined, an estimate of the location of the true zero crossing can be obtained by averaging the locations of same-signed zero crossings in the cluster. It can be shown* that the *location distribution* associated with this strategy is approximately Gaussian with a standard deviation that is inversely proportional to the slope of the sinewave at the true zero crossing.

Peaks in the noisy waveform usually do not coincide exactly with the peak of the stimulus sinewave. We used the position of the peak in the noisy waveform to estimate the location of the stimulus peak. We compiled *location distributions* for peaks using Monte Carlo simulations running on a SUN 3/50 workstation. We also examined the location distributions for centroids using computer simulations. In both cases, the location distributions were approximately Gaussian in form.

In a forced-choice disparity-detection trial, the appropriate decision variable is the difference in the estimated locations of matched features in the two eyes. Since the monocular location distributions are approximately Gaussian, the difference distribution is also Gaussian. Accuracy can be characterized by d', the mean of the decision variable divided by its standard deviation:

$$d' = 2d/\sqrt{(\sigma_L^2 + \sigma_R^2 - 2\rho\sigma_L\sigma_R)},$$

where d is the monocular offset (equal but opposite in the two eyes, see Fig. 9), σ_L and σ_R are the standard deviations of the left and right location distributions and ρ is the correlation between noise fluctuations in the two eyes. (The term in ρ is subtracted because the decision variable is a difference of two distributions.) In this equation, $2d$ is disparity. If we define threshold disparity D_t to correspond to a d' value of one as in our experiments:

$$D_t = \sqrt{(\sigma_L^2 + \sigma_R^2 - 2\rho\sigma_L\sigma_R)}. \quad (3)$$

Effect of frequency. When the monocular contrasts are equal, we assume that $\sigma_L = \sigma_R$ and designate both by σ. From equation (3), disparity threshold is then proportional to σ:

$$D_t \propto \sigma. \quad (4)$$

For a given input contrast (i.e. signal level) two factors influence the standard deviation of the location distributions: signal-to-noise ratio and sampling density (i.e. number of sampling elements per cycle). Assuming the channels are identical in these respects and that there are channels with peak frequencies matched to the stimulus gratings, the standard deviations of the location distributions will be a constant fraction of a cycle. This constancy is equivalent to disparity thresholds that are inversely proportional to spatial frequency and applies equally well to zero crossings, peaks and centroids. Our sinewave data (Fig. 3) are consistent with this relation for spatial frequencies below 3 c/deg. The assumption of equal signal-to-noise ratio across channels, however, is questionable given the decline in the contrast-sensitivity

*The probability of a zero crossing of a given polarity between adjacent samples of a noisy neural waveform is equal to the probability that one has a negative value times the probability that the other is positive. Near its zero crossings, $A\sin(kx)$ can be approximated by Akx. When Gaussian noise is added, the probability that a sampled value at x_0 is positive is equal to the probability that Akx_0 plus a sample of Gaussian noise is greater than zero. In other words, the value is positive if the Gaussian sample is greater than $-Akx_0$. Therefore, the probability of a positive value is a cumulative normal distribution. Similarly, the probability that the adjacent value is negative is one minus a cumulative normal. The product of a cumulative normal times one minus a cumulative normal is exceedingly well approximated by a Gaussian distribution with mean at $x = 0$ and standard deviation proportional to $1/kA$. In a given stimulus presentation, one or more such zero crossings will be present in a cluster. An estimate of the location of the corresponding stimulus zero crossing is obtained as the average of the locations of same-polarity zero crossings in the cluster. The standard deviation of this *location distribution* is also proportional to $1/kA$, but smaller by a factor of $\sqrt{n}$ where n is the average number of same-signed zero crossings in the cluster.

function at low spatial frequencies. The assumption of multiple channels in the range of low spatial frequencies is also questionable (cf. Campbell, Johnstone & Ross, 1981).

The effect of contrast. In the case of zero crossings, our analysis showed that the standard deviation of the location distribution is inversely proportional to the amplitude of the sinusoidal modulation in the neural image and hence to stimulus-grating contrast.* Therefore, the zero-crossing model predicts that disparity threshold is inversely proportional to contrast. This is inconsistent with the inverse square-root relation that we found.

A similar interpretation holds if we take the feature underlying disparity detection to be the luminance gradient in the stimulus rather than zero crossings in the neural image associated with a channel. The maximum luminance gradient of a sinewave is located at its zero crossings and is proportional to the product of contrast and spatial frequency. If it is the critical feature governing disparity detection, then disparity thresholds should show the same functional dependence on spatial frequency and contrast. Our data indicate that this is not so, Heckmann and Schor (1989) have studied the possible role of luminance gradients in stereopsis in detail. They have measured disparity thresholds for compound gratings with varying phase relations. Consistent with our findings, their data indicate that disparity thresholds are not determined by luminance gradients.

Figure 10A plots standard deviation as a function of signal-to-noise ratio (s/n) for the centroid simulations. Since standard deviation is proportional to disparity threshold (equation 4), and s/n is proportional to contrast (assuming constant noise amplitude), the graph amounts to a plot of disparity threshold vs contrast. Each standard deviation was taken from a distribution compiled from 1000 simulated trials. The

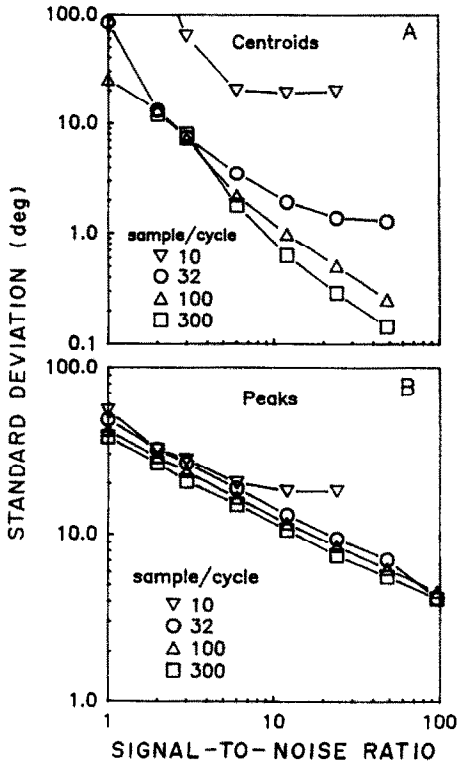

Fig. 10. Results of computer simulations. The ordinate is the standard deviation (SD) of the distribution of positions of centroids or peaks in noise-perturbed sinewaves. Each point is based on 1000 simulated trials. The SD is for monocular localization and has units of degrees of a cycle. Assuming the monocular contrasts are equal, disparity threshold is proportional to monocular SD. The abscissa is signal-to-noise ratio (s/n), i.e. the ratio of sinewave amplitude to the SD of the Gaussian noise. Assuming constant noise level, s/n is proportional to sinewave contrast.

separate curves are for different spatial sample densities (i.e. number of channel receptive fields per sine-wave cycle). Figure 10A shows that for low sample densities, the centroid model predicts a curvilinear relation between disparity threshold and contrast, inconsistent with our data. While portions of these curves can be approximated by straight lines, we were unable to find a partial curve, covering a large enough range of s/n that was well fit by an inverse-square-root law. For high sample densities, the curves are straighter but too steep (slopes near -1) to fit the inverse square-root law.

Figure 10B shows standard deviation as a function of s/n for peaks. For sample densities greater than about 10, the simulation results are well fit by straight lines with slopes very close to -0.5 (range from -0.483 to -0.514). Clearly, the peak model provides a better fit to our contrast data than either the zero-crossing or centroid model.

*Near its zero crossings, $A\sin(x)$ can be approximated by Ax. The reciprocal relation between the standard deviation of the location distribution for zero crossings and sinewave amplitude is determined by this product relation; a criterion deviation of the function from zero is given by $Ax = \text{constant}$ or $x \propto 1/A$. This "trading relation" between amplitude and position holds even if a nonlinear transformation is applied to $A\sin x$ prior to the addition of noise. Therefore, the zero-crossing model predicts inverse proportionality between disparity threshold and contrast even in the presence of the sort of nonlinear compression proposed by Legge and Foley (1980).

Watt and Morgan (1985) also used computer simulations to model accuracy of spatial localization. They used uniform rather than Gaussian noise. We repeated some of our simulations with uniform noise and found results consistent with their's. Plots of standard deviation vs s/n for the two types of noise are qualitatively similar. There were some quantitative differences e.g. for the peaks, slopes were near -0.4 for uniform noise and -0.5 for Gaussian noise.

The effect of unequal contrast. Adopting a model, such as the peak model, in which the standard deviation of the location distribution is inversely proportional to the square root of grating contrast, we can express σ_L and σ_R in equation (3) in terms of left and right contrasts as $1/\sqrt{C_L}$ and $1/\sqrt{C_R}$. Let C_R be constant and C_L vary. The contrast ratio is represented by $r = C_R/C_L$. From equation (3), we obtain:

$$D_t \propto (1/\sqrt{C_R})[1 + r - 2\rho\sqrt{r}]^{1/2}. \qquad (5)$$

This equation gives threshold disparity as a function of the contrast ratio r for a fixed value of contrast C_R. However, a value of the noise correlation ρ must be chosen before the relation can be plotted. We used a least-squares method to choose values of ρ maximizing the fit of equation (5) to our data sets. Figure 11 replots the 0.5 c/deg unequal contrast data for our two subjects from Fig. 7. Threshold disparities have been normalized by the value for the equal-contrast case. For each subject, sets of data with constant contrasts of 0.25 and 0.125 are shown as different symbols. The solid lines through the data represent the best-fitting versions of equation (5). For subject DR, the curve is characterized by a noise correlation of 0.986. For KD, the correlation is 0.976. Noise correlations at 2.5 c/deg were a little lower—0.974 for DR and 0.891 for KD. The solid lines provide only a rough fit to the data and do not fully represent the accelerating growth of threshold with increasing contrast ratio.

Best values of the noise correlation ρ were very high. For comparison, the dashed lines in Fig. 11 show the predictions for uncorrelated noise, i.e. $\rho = 0$. Such high correlations imply that a largely common source of noise on the left and right channels limits disparity detection. Presumably, this noise would be added close to the site of disparity computation. The differencing operation inherent in stereo, performed in the presence of highly correlated noise, means that disparity detection enjoys the improved

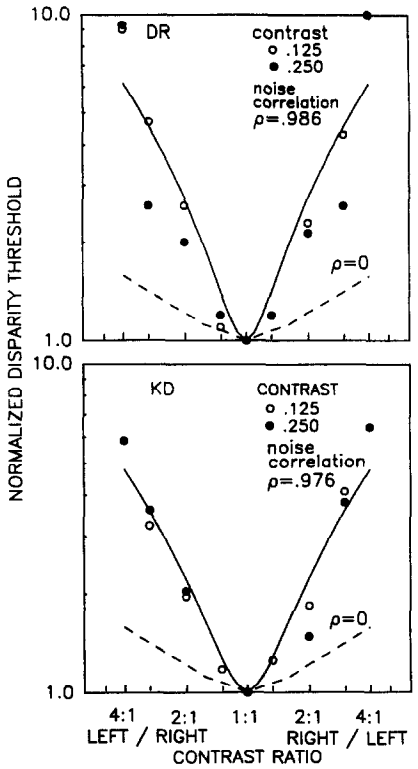

Fig. 11. Disparity thresholds as a function of contrast ratio at 0.5 c/deg are replotted from Fig. 7. Thresholds have been normalized by the threshold disparity for the equal-contrast condition, i.e. a ratio of 1:1. The solid curves through the data were obtained from equation (5) by selecting values of the noise correlation ρ that yielded the best fit. The dashed curves show the corresponding plots for uncorrelated noise ($\rho = 0$). Data are shown for observers DR and KD.

signal-to-noise ratio of a differential amplifier. Westheimer (1979) has already suggested that neural processing underlying stereopsis might be analgous to a differential amplifier.

In this section, we have evaluated disparity-threshold predictions of multiple-channels stereo models based on zero crossings, peaks and centroids. The three models can account for the effect of frequency below 3 c/deg, but not for the idiosyncratic effects at higher spatial frequencies. Neither the zero-crossing model nor the centroid model accounts for the dependence of disparity threshold on contrast. The peak model does predict the observed inverse-square-root relation. Finally, the effect of enequal monocular contrasts on threshold disparity can be accounted for if the limiting noise in the two eyes is highly correlated.

Acknowledgements—Preliminary reports of these findings were presented at the annual meeting of the *Association for Research in Vision and Ophthalmology*, 1988, and at the Rank Prize Funds conference on *Biological and Engineering*

Aspects of Visual Hyperacuity and Depth Perception, held at Trinity Hall, Cambridge, England, 9–11 January, 1984. We thank John M. Foley for comments on the manuscript. We thank Gary S. Rubin for help with apparatus and procedures, and Andrew Luebker for help with several of the figures. This research was supported by U.S. Public Health Service Grants EY02857 and EY02934 to Gordon E. Legge.

REFERENCES

Berry, R. N. (1948). Quantitative relations in vernier, real depth and stereoscopic depth acuities. *Journal of experimental Psychology, 38,* 708–721.

Blakemore, C. & Hague, B. (1972). Evidence for disparity detecting neurons in the human visual system. *Journal of Physiology, London, 225,* 437–455.

Burton, G. J. (1981). Contrast discrimination by the human visual system. *Biological Cybernetics, 40,* 27–38.

Campbell, F. W. & Robson, J. G. (1968). Application of fourier analysis to the visibility of gratings. *Journal of Physiology, London, 197,* 551–566.

Campbell, F. W., Johnstone, J. R. & Ross, J. (1981). An explanation for the visibility of low-frequency gratings. *Vision Research, 21,* 723–730.

Carlson, C. & Cohen, R. (1978). A non-linear spatial frequency signal detection model for the human visual system. *Journal of the optical Society of America, 68,* 1379.

Felton, T. B., Richards, W. & Smith, R. A. Jr. (1972). Disparity processing of spatial frequencies in man. *Journal of Physiology, London, 225,* 340–362.

Frisby, J. P. & Mayhew, J. E. W. (1978). Contrast sensitivity function for stereopsis. *Perception, 7,* 423–429.

Green, D. M. & Swets, J. A. (1974). *Signal detection theory and psychophysics*. Huntington, NY: Krieger.

Halpern, D. L. & Blake, R. (1988). How contrast affects stereoacuity. *Perception, 17,* 483–495.

Heckmann, T. & Schor, C. M. 1(1989). Is edge information for stereoacuity spatially channelled? *Vision Research 29,* 593–607.

Julesz, B. (1971). *Foundation of cyclopean perception*. Chicago, IL: University of Chicago Press.

Legge, G. E. (1979). Spatial frequency masking in human vision: Binocular interactions. *Journal of the optical Society of America, 69,* 838–847.

Legge, G. E. (1984). Binocular contrast summation—II. Quadratic summation. *Vision Research, 24,* 385–394.

Legge, G. E. & Foley, J. M. (1980). Contrast masking in human vision. *Journal of the optical Society of America, 70,* 1458–1471.

Legge, G. E. & Kersten, D. (1983). Light and dark bars: Contrast discrimination. *Vision Research, 23,* 473–483.

Levi, D. M. & Klein, S. A. (1983). Spatial localization in normal and amblyopic vision. *Vision Research 23,* 1005–1017.

Lit, A., Finn, J. P. & Vicars, W. (1972). Effect of target background luminance contrast on binocular depth discrimination at photopic levels of illumination. *Vision Research, 12,* 1241–1251.

Marr, D. & Poggio, T. (1979). A computational theory of human stereo vision. *Proceedings of the Royal Society, London. B204,* 301–328.

Mayhew, J. E. W. & Frisby, J. P. (1981). Psychophysical and computational studies towards a theory of human stereopsis. *Artificial Intelligence, 17,* 349–385.

Morgan, M. J. & Regan, D. (1987). Opponent model for line interval discrimination: Interval and vernier performance compared. *Vision Research, 27,* 107–118.

Ogle, K. N. & Weil, M. P. (1958). Stereoscopic vision and the duration of the stimulus. *American Archives of Ophthalmology, 59,* 4–17.

Poggio, G. F. & Poggio, T. (1984). The analysis of stereopsis. *Annual Reviews, Neuroscience, 7,* 379–412.

Rubin, G. S. (1983). Suppression and summation in binocular pattern vision. Ph.D. Thesis, Department of Psychology, University of Minnesota.

Schor, C. M. & Wood, I. (1983). Disparity range for local stereopsis as a function of luminance spatial frequency. *Vision Research, 23,* 1649–1654.

Simons, K. (1984). Effects of stereopsis on monocular vs binocular degradation of image contrast. *Investigative Ophthalmology and Visual Science, 25,* 987–989.

Stigmar, G. (1971). Blurred visual stimuli. II. The effect of blurred visual stimuli on vernier and stereo acuity. *Acta Opththalmologica, 49,* 364–378.

Watson, A. B. & Pelli, D. G. (1983). Quest: A Bayesian adaptive psychometric method. *Perception and Psychophysics, 33,* 113–120.

Watt, R. J. & Morgan, M. J. (1983). The recognition and representation of edge blur: Evidence for spatial primitives in human vision. *Vision Research, 23,* 1565–1577.

Watt, R. J. & Morgan, M. J. (1985). A theory of the primitive spatial code in human vision. *Vision Research, 25,* 1661–1674.

Westheimer, G. (1978). Spatial phase sensitivity for sinusoidal grating targets. *Vision Research, 18,* 1073–1074.

Westheimer, G. (1979). Cooperative neural processes involved in stereoscopic acuity. *Experimental Brain Research, 36,* 585–597.

Westheimer, G. & McKee, S. P. (1980a). Stereoscopic acuity with defocus and spatially filtered retinal images. *Journal of the optical Society of America, 70,* 772–777.

Westheimer, G. & McKee, S. P. (1980b). Stereogram design for testing local stereopsis. *Investigative Ophthalmology and Visual Science, 19,* 802–809.

Wilson, H. R. (1980). A transducer function for threshold and suprathreshold spatial vision. *Biological Cybernetics, 38,* 171–178.

Wilson, H. R. (1986). Responses of spatial mechanisms can explain hyperacuity. *Vision Research, 26,* 453–469.

Wood, I. C. J. (1983). Stereopsis with spatially-degraded images. *Ophthalmic and Physiological Optics, 3,* 337–340.